

Grasping with Soft Hands

M. Bonilla¹, E. Farnioli^{1,2}, C. Piazza¹, M. Catalano², G. Grioli², M. Garabini¹, M. Gabiccini^{1,2,3}, A. Bicchi^{1,2,4}

Abstract—Despite some prematurely optimistic claims, the ability of robots to grasp general objects in unstructured environments still remains far behind that of humans. This is not solely caused by differences in the mechanics of hands: indeed, we show that human use of a simple robot hand (the Pisa/IIT SoftHand) can afford capabilities that are comparable to natural grasping. It is through the observation of such human-directed robot hand operations that we realized how fundamental in everyday grasping and manipulation is the role of hand compliance, which is used to adapt to the shape of surrounding objects. Objects and environmental constraints are in turn used to functionally shape the hand, going beyond its nominal kinematic limits by exploiting structural softness.

In this paper, we set out to study grasp planning for hands that are simple - in the sense of low number of actuated degrees of freedom (one for the Pisa/IIT SoftHand) - but are soft, i.e. continuously deformable in an infinity of possible shapes through interaction with objects. After general considerations on the change of paradigm in grasp planning that this setting brings about with respect to classical rigid multi-dof grasp planning, we present a procedure to extract grasp affordances for the Pisa/IIT SoftHand through physically accurate numerical simulations. The selected grasps are then successfully tested in an experimental scenario.

I. INTRODUCTION

During the past thirty years, the problem of autonomous robotic grasping has been one of the most widely investigated. For well known scenes and object models, pre-programming of autonomous grasping and manipulation tasks may be an option. Toward this goal, several approaches have been proposed to define the optimal finger placement on the object, either based on some geometric [1] or force [2], [3] grasp quality measures, specifically tailored to convex objects [4], with optimal on-line contact adjustments [5], and also generalized to non-convex objects [6]. Perhaps because of the fragility of the mechanics of most robot hands, a multitude of the planning methods were thought for interactions between the hand and the object that only occurred at the fingertips, limiting contacts with other parts of the hand and avoiding contacts with the rest of the environment at all.

This “timid” approach to manipulation generated by rigidity and fragility of the hand has been recently challenged by the introduction of adaptable, underactuated and/or soft hands. Devices such as the underactuated RobotIQ hand [7], the RBO and RBO 2 hands [8], [9], the iHY hand [10] and the Pisa/IIT SoftHand [11], are designed to be much simpler,

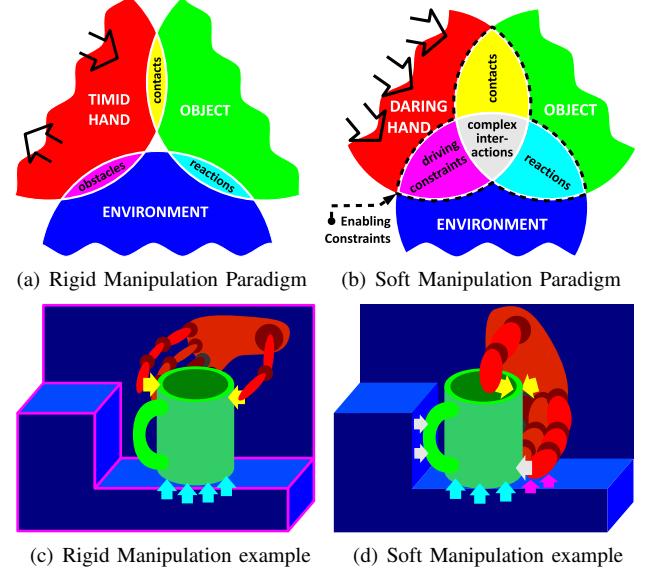


Fig. 1. Paradigm shift in manipulation, from rigid manipulation (left) to soft manipulation (right). Primary colors identify the scenario main actors: red for the robotic hand, blue for the environment, green for the target object. Secondary colors codify simple interactions between the actors: yellow for hand-object, cyan for object-environment and magenta for environment-hand. Finally, complex interactions, which involve all the three actors at the same time, are white colored. Refer to text for a deeper description.

and much more robust with respect to the whole interaction process. This allows to use these hands in more “daring” interactions with the objects in the environment, using their full surface for enveloping grasps, and exploiting objects and environmental constraints to functionally shape the hand, going beyond its nominal kinematic limits by exploiting structural softness.

The differences between a rigid and soft approach to manipulation are sketched in Fig. 1. In the classical paradigm (cfr. panel (a)), the planner searches for suitable points on the object that generate a nominal grasp of good quality, and for trajectories that can bring there the fingertips while avoiding contacts of the hand with the environment. In the example of panel (c), to grasp the green cup while avoiding the wall on the left the planner has to find a path in a narrow passage. However, soft manipulation subverts this scheme (panel (b)). In the example of panel (d), hand-object, object-environment and hand-environment contacts are not avoided but rather sought after and exploited to shape the hand itself around the object.

The set of all possible physical interactions between the hand, the object and the environment, which define the hand-object functional interaction, will be referred to as the set of *Enabling Constraints*. The analysis of such

¹Research Center “E. Piaggio”, Università di Pisa, Largo Lucio Lazzarino 1, 56122 Pisa, Italy

²Department of Advanced Robotics, Istituto Italiano di Tecnologia, Via Morego 30, 16163 Genova, Italy

³Department of Civil and Industrial Engineering, Università di Pisa, Largo Lucio Lazzarino 1, 56122 Pisa, Italy

⁴Department of Information Engineering, Università di Pisa, Via Caruso, 2, 56122 Pisa, Italy

possibilities constitute a rather new challenge for existing grasping algorithms: adaptation to totally or partially unknown scenes remains a difficult task, toward which only some approaches have been investigated so far. Some of them are model-free and propose geometrical features which indicate good grasps [12], [13], some others evaluate also topological object properties such as holes [14]. Typically, grasps are ranked on a fixed list of suitable hypotheses, do not require supervised learning, but do not adapt over time. Other methods are based on learning the success rate of grasps given some descriptor extracted from sensor data, either evaluated on a real robotic system [15], [16], or on simulated sensor data [17], [18].

Moreover, beside vision-based methods, hand compliance offers the real possibility to use tactile exploration for 3D reconstruction of unknown environments and objects. Tactile sensing can solve some severe limitations of computer vision, such as sensitivity to illumination and limited perspective. As an example, a combined procedure based on dynamic potential fields, that aims at reconstructing 3D object models, which are then used for grasp planning and execution was presented in [19] and recently extended in [20].

In this paper, we consider planning grasps with hands that are simple – in the sense of low number of actuated degrees of freedom, e.g. one for the Pisa/IIT SoftHand – but are soft, i.e. continuously deformable in an infinity of possible shapes through interaction with objects. We present a first approach to the study of this novel kind of manipulation, based on an accurate simulation tool for the SoftHand, developed using the multi-body system software ADAMS [21]. A batch simulation set-up was created and used to perform the automatic creation of a database of grasp affordances for the Pisa/IIT SoftHand and a set of kitchenware objects. The method is related to that followed with simulators such as GraspIt! [22], Open-Rave [23] and OpenGRASP [24], although the softness of the hand introduces a new vista on the problem.

To stress the differences between the rigid and soft manipulation paradigms, Section II presents some of the benefits of using Soft Hands to grasp objects. Section III recalls the mathematical model of the SoftHand after which the simulation tool, presented in Section IV, has been developed. Section V presents the automated simulation batch environment, that led to the results presented in section VI. Finally conclusions are drawn in Section VII.

II. A NEW SET OF POSSIBILITIES

By observing the way humans use their real hands, it is possible to realize that, in everyday grasping and manipulation, the role of hand compliance is fundamental. In the first place it is used to adapt to the shape of the hand surroundings: both the target object and the rest of the environment. On the other hand, it is important to notice how the objects and the environment constraints are used, in turn, to functionally shape the hand, going beyond its nominal kinematic limits by exploiting its structural softness.

Although one could ascribe such levels of dexterity to the high levels of sensory-motor capabilities of the human hand itself, it is astounding to compare the performance of the human naked hand with that of a person using a simple robot



Fig. 2. A human hand grasping a cup with three different approaches (top panels) and the same grasps reproduced with the Pisa/IIT SoftHand (bottom panels).



Fig. 3. The Pisa/IIT SoftHand mounted on a human arm.

hand, as the Pisa/IIT SoftHand arm-mounted device shown in Fig. 3.

Thanks to its under-actuated mechanisms the SoftHand is capable to grasp several number of objects by matching to their shape. These combination of simplicity, adaptivity and robustness lets the person experiment in a very natural way with the robotic hand, and soon achieve a level of performance comparable, often similar, to that obtained with their true hands. This achievement is obtained despite the presence of just one degree of actuation on the mechanism and an almost total lack of tactile feedback. Fig. 2, shows three very different ways to grasp a cup, implemented with both the naked hand and the SoftHand.

The SoftHand can substantially match the grasping performance of the human hand thanks to its possibility of exploring and exploiting the *Enabling Constraints* that define, at a very basal level, the problem of grasping and manipulation.

As a further example, consider Fig.s 4, where the combined action of adaptability and robustness allow the user to manipulate and interact with both the environment and the object at the same time, in a complex way (refer also to Fig. 1). Exploiting all the physical constraints that are external with respect to the hand itself: walls, surfaces and edges, force closures of the object between the hand and the environment can be obtained and used to generate simple and effective manipulation tasks, in this case sliding and pivoting



Fig. 4. A person with the arm-mounted SoftHand can seamlessly execute also difficult manipulation tasks which involve combined interactions between hand, object and the environment.

a book.

III. MODEL OF THE PISA/IIT SOFTHAND

As an example of the new advantages introduced for the soft manipulation paradigm, we investigate how to plan grasps for the Pisa/IIT SoftHand.

Fig. 12 shows that despite the fact the hand is always driven by the same closing command for any object, the final grasps are characterized by different joint configurations, automatically obtained thanks to the adaptability of the hand. The only variables needed to synthesize grasp remain those ones describing the wrist pose. In next sections we will present a randomized investigation method, in order to discover sets of hand/object configurations bringing to the grasp. As follows from previous discussions, the dynamic evolution of the system play a key role, from the pre-grasp phase until a stable grasp is achieved. Hence, starting from the kinematic model of the hand, extensively presented in [11], we developed a dynamic simulation tool in ADAMS. The main equations to be considered in the simulator come from the kineto-static model of the Pisa/IIT hand, which can be described by the following

$$s = Rq, \quad (1)$$

$$\tau = R^T \eta - K_q q. \quad (2)$$

In eq. (1) variable $s \in \mathbb{R}$ describes the displacement of the extremities of the actuation tendon, while $q \in \mathbb{R}^{19}$ is the joint displacement vector, comprising 5 revolute joints for the abduction movement, and 14 soft roll-articular (SR) joints for the flex/extension movement of the fingers. The map between the two variables is the so called *adaptive synergy matrix* $R \in \mathbb{R}^{1 \times 19}$. From eq. (1), by kineto-static duality, eq. (2) follows, where $\eta \in \mathbb{R}$ is the motor torque, and $\tau \in \mathbb{R}^{19}$ is torque vector at the joint level. The *joint stiffness matrix* $K_q \in \mathbb{R}^{19 \times 19}$ is introduced to properly consider the effect of the joint elastic band on the net torque.

IV. SIMULATOR IMPLEMENTATION

After the CAD models of the parts composing the hand have been imported, a virtual link is placed between the two real ones, Fig. 5(a). Each real part is connected to the virtual one by virtue of a revolute joint, Fig. 5(b). Finally, the coherence between the movements of the simulated SR joint and the real one is assured by introducing a gearwheel-type constraint, Fig. 5(c).

In order to properly describe the behavior of the Pisa/IIT SoftHand, it is important to take also into account: (i) the kinematic constraints imposed by the tendon routing, (ii) the

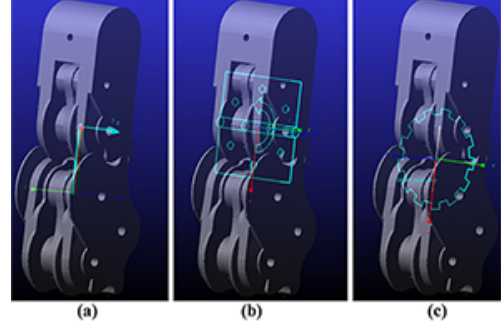


Fig. 5. Implementation of the SR joint in ADAMS: a virtual link is introduced between the two elements (a); a revolute joint connects the virtual link with each real parts (b); a gear-wheel constraint is imposed between the two revolute joints (c).

effects of the elastic bands at the joints since, as follows from (2), both the terms contribute to the net joint torques. The effect of the motor torque was introduced in ADAMS by imposing the desired torque on each joint, considering both the motor torque curve versus time, and the adaptive synergy matrix R . The contribution of the elastic bands is introduced in the model using the ADAMS rotational springs. By properly tuning the damping term in the ADAMS model of springs, the Coulomb friction at the joints is modeled, this has also the beneficial effects of avoiding unphysical oscillations of the simulation if not present.

Regarding to Fig. 1, the *Enabling Constraints* exploited in the next set of simulations are *contacts* and *reactions*. It means that all contact interactions among object, table and hand geometries are enabled. In order to reduce the set of possible grasp configurations to explore, the inclusion of *driving constraints* is kept as a future work.

V. BATCH SIMULATION SETUP

In order to perform a large set of simulations for the Pisa/IIT SoftHand, the ADAMS model was fully parameterized via a template script. Design parameters like object inertia, contact parameters and joint stiffness and friction, were properly chosen to mimic the real hand as closely as possible, they do not need to be modified during the simulation campaign. The sole parameters to be modified are those defining the pose of the hand with respect to the object. To this aim, and to keep the number of simulations reasonably low, without sacrificing the quality of the results, a certain strategy had to be devised.

The first strategy we attempted was an extensive investigation sampling four of the six DoFs necessary to define the position and orientation of the palm frame with respect

to the object frame. More in detail, the position of the origin of the palm frame was parameterized in spherical coordinates (radius, azimuth and elevation). The normal to the palm frame always points toward the center of the sphere which coincides with the origin of the object frame. The remaining DoF is the rotation of the hand frame around the normal. With this strategy a large number of attempts were unsuccessful because, in the starting configuration, the hand was either already interpenetrating the object, or excessively far from it. In the first case, the simulation was skipped, because of the non-feasible condition, while in the latter the object was out of reach or the ejection of the object occurred. The main reason is that a sphere is not a good generalization of many object geometries, such as a pot or a cup.

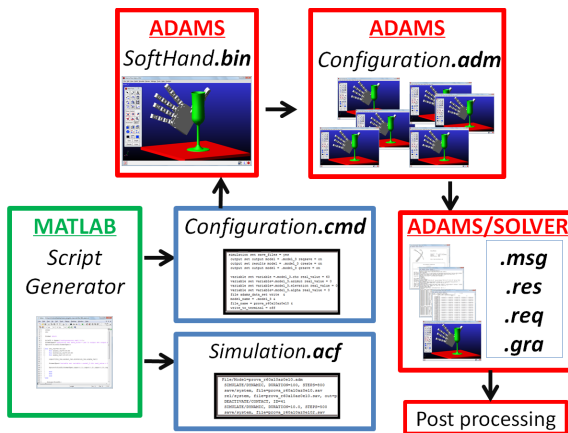


Fig. 6. A flow chart of the use of ADAMS and MATLAB for running batch simulations. In MATLAB, a *.cmd* file is used to define the hand configurations in which attempting the grasp. By loading this file in ADAMS, together with a *.bin* file containing the object/hand model, we can obtain a file (*.adm*) for each configuration. Running the *.acf* file, the *.adm* ones are read, performing the simulations in batch mode. Simulation variables (joint angles, contact forces, etc...) are available in the exit files (*.msg*, *.res*, *.req*, *.gra*) for post-processing operations.

This suggested us to redesign the strategy taking into account the geometry of the object, focusing the attention on the mesh describing the shape of the object.

The mesh of the object to be grasped was imported in MATLAB, and the points of and the normal vectors to the surface were extracted. For 50 randomly selected points of the mesh, the pose of the hand frame was chosen positioning its origin 5 mm (coming from observations of real experiments) outside the surface mesh along the outward normal. The normal to the palm was aligned with the normal to the object at the point, but with opposite direction (the palm always faces the object). Finally, 8 configurations were selected rotating the hand around its normal axis. The 400 palm configurations obtained were put on a test for achieving a stable grasp. Fig. 6 represents a scheme of the flow chart for running batch simulations.

The results achieved after this first investigation step are represented, for the case of the pot, in Fig. 9, where green frames represent successful configurations (stable grasp achieved), red frames the unsuccessful ones. In order to evaluate if a grasp is stably achieved, all the simulations were split into two parts. In the first part the object to be grasped lies on a plane, orthogonal to the gravity vector, in order to hold it on without over-constraining it. No contact

was set up between the hand and the table to do not preclude any possible approach direction. This simulation part is three seconds long, that is approximately one second longer than the time of free closure of the hand. Later, starting from the final configuration of the first simulation and keeping active the hand motor torque, a two seconds long simulation is performed removing the table. Afterwards, the velocity of the object is read from the output files, and the grasp is rated as achieved and stable if the velocity is smaller than a tolerance value.

From the results of the first set of simulations, the points that brought to a stable grasp were extracted, and their neighbourhood was further investigated. This research was performed by randomly choosing 10 of the 40 closest points on the mesh, around the successful one. For each new point, again 8 rotations around the palm normal were considered to attempt the grasp.

VI. SIMULATION RESULTS

The free closure movement of the Pisa/IIT SoftHand obtained with ADAMS is shown in Fig. 7. As explained in Sec. IV, the hand model considers both the tendon routing, eq. 1, and the elastic bands at the joints, eq. 2. The reader can find a deeper analysis about the kineto-static model of the hand in [11].

In our simulation campaign we used everyday objects: a cup, a pot, a colander and a plate, see Fig 8. For the cup example, Fig. 9 shows: a) the points composing the object mesh, b) successful (green) and unsuccessful (red) grasps configurations after the first 400 simulations, c) the result for all tested hand postures and d) all successful configurations.

In order to validate the dynamic behaviour of the simulator and to put the obtained results on a test, some successful hand palm configurations were also implemented with the Pisa/IIT SoftHand prototype. A KUKA lightweight robot was used to exactly replicate the hand/object configuration suggested by the simulation. A comparison snapshot sequence for the pot and the colander is shown in Fig.s 10 and 11.

In TABLES I and II some numerical results of the simulations are summarized. Specifically, in TABLE I, for every object we list: (i) successful postures, the number of palm frame configurations bringing to a stable grasp, (ii) successful points, the number of unique origin positions of the hand frame with possibly multiple orientations, (iii) clouds, number of neighbourhoods investigated, (iv) best cloud, maximum number of successful grasps in a cloud. As we can see, the best result in terms of number of grasp achieved, as well as in terms of individual successful points, is obtained for the pot. However, the best cloud is found for the plate.

In TABLE II, some simple quality indices are listed. In particular, the *cloud quality* (CQ) index reports the highest percentage of stable grasps achieved in the tested clouds. The CQ index is computed as

$$CQ = \frac{g_b}{c_b} 100, \quad (3)$$

where g_b is the number of stable grasp achieved and the c_b is the number of hand palm configurations tested, both considered for the best cloud. The *closure* index (CI) is a measure of how much the hand is closed at the end of the

	successful postures	successful points	clouds	best cloud
Cup	30	13	8	10
Pot	138	41	16	35
Colander	21	6	2	14
Plate	112	29	10	37

TABLE I

Simulation results: (i) number of initial postures leading to a successful grasp, (ii) number of successful individual starting points for the hand placement, (iii) number of clouds studied and (iv) maximum number of successful configurations found in a cloud (best cloud).

	CQ Index %	Closure Index (min-max)%	Net Force (N)
Cup	11.3	40-73	1-57
Pot	39.7	48-68	2-36
Colander	15.9	54-67	11-52
Plate	42.1	57-69	6-28

TABLE II

Simulation results and quality measures. *Cloud Quality* (CQ) index is the percentage of stable grasp achieved, with respect to the number of postures attempted, in the best cloud. *Closure* index (CI) is how much the hand is near to the complete closure configuration, minimum and maximum values found for all the successful grasps are reported. *Net Force* (NF) measures the amount of contact forces exceeding the weight of the object (minimum and maximum).

simulation. In TABLE II the minimum and maximum values found for each object are shown. This index is computed as

$$CI = \frac{100}{n_{q_c}} \sum_{i=1}^{n_{q_c}} \frac{q_{f_i}}{q_{c_i}}, \quad (4)$$

where q_{f_i} is the final configuration of the i^{th} joint during the grasp, q_{c_i} is the maximum reachable value allowed by the mechanical constraints for the i^{th} joint, and n_{q_c} in the number of flex-extension joints.

The *Net Force* (NF) is a measure of the amount of internal forces produced in the grasp by the finger limbs. It is computed as

$$NF = \left(\sum_{i=1}^c f_{c_i}^T f_{c_i} - w_o^T w_o \right)^{\frac{1}{2}}, \quad (5)$$

where c is the number of contact points, f_{c_i} is the force at the i^{th} contact point, and w_o is the weight of the grasped object.

As it is evident from table II, the best *cloud quality* (CQ) index is achieved for the plate. However, also high values of *closure index* are realized when grasping the plate. This result can be explained by taking into account that all the tests were performed with the same torque vs time motor curve. In some cases, especially for the plate, results show that the amount of motor torque is enough to overcome the friction and to bring the hand in a closure configuration. The greatest amount of the NF index, is realized to grasp

the colander. The explanation for this result is, again, an excessive level of motor torque, in particular with respect to the low weight of the object. The relevant difference between the minimum and the maximum value of the NF index for all the objects can be explained considering that the palm force is not measured in the simulator. This implies that high values of the NF index correspond to grasps in which the interaction forces are primarily executed by the fingers, low values correspond to grasps that mainly involve the palm.

Generally speaking, the not excellent results of the colander (just 2 clouds and 21 successful configurations) can be explained with the difficulty of randomly selecting points near to the upper edge or the handles. Moreover, the meshes of the objects, obtained from CAD files, are characterized by the presence of (nominally) normal vectors that, indeed, are not orthogonal to the object surface. In some cases, an hand/object interpenetration can occur, caused by a palm normal orientation not orthogonal to the object surface, and the selected point (potentially good) is discarded. For similar reasons, we can consider the cup and the pot as being penalized. Potentially, more points could be have been found on their handle having a better representation of the mesh points and of the normal vectors to the surface.

VII. CONCLUSION

This paper moves a first step in the direction of studying grasp planning for simple soft hands, imbued with the capabilities of comply with the manipulated object within, and together with, the environment.

Some considerations extracted from the observation of humans to execute simple and more complex tasks, using both their hands and an arm-mounted robot hand, led us to suggest a possible change of paradigm in grasp planning that this setting brings about. After that, we presented a procedure to extract grasp affordances for the Pisa/IIT SoftHand, built upon a physically accurate numerical simulations system that was purportedly implemented. This allowed to select a set of possible grasps that were then successfully tested in an experimental scenario. Despite this early results, much work remains to be done to sharpen the grasp search and to abstract learned grasps between different objects. Although the reported results only scratch the surface of the wholly new problem of soft manipulation planning, however, our results indicate that soft manipulation can be a viable solution for obtaining stable and robust robot grasps.

ACKNOWLEDGMENTS

This work is supported by the EC under the CP-IP grant no. 600918 “PaCMan”, within the FP7-ICT-2011-9 program “Cognitive Systems”, ERC Advanced Grant no. 291166 “SoftHands” - A Theory of Soft Synergies for a New Generation of Artificial Hands-, under grant agreements no. 611832 “Walk-Man” and by CONACYT through the scholarship 266745/215873.

REFERENCES

- [1] C. Ferrari and J. Canny, “Planning optimal grasps,” *Proceedings 1992 IEEE International Conference on Robotics and Automation*, pp. 2290–2295, Jan. 1992.
- [2] D. Prattichizzo, J. Salisbury, and A. Bicchi, “Contact and grasp robustness measures: Analysis and experiments,” *Experimental Robotics IV*, Jan. 1997.

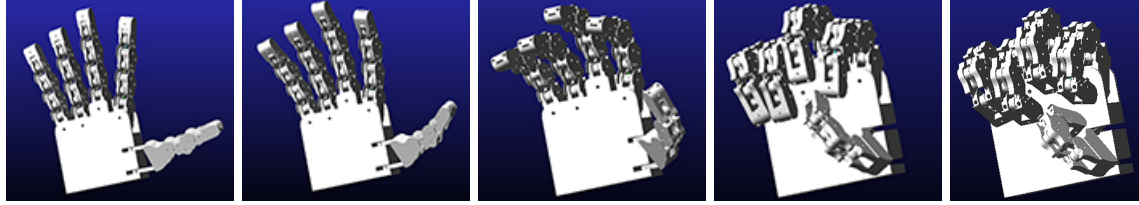


Fig. 7. Sketches of the free closure movement of the Pisa/IIT SoftHand in ADAMS simulation. Since there is neither object nor environment, the movement of the hand is described by the synergistic model of actuation described in eq. (1).

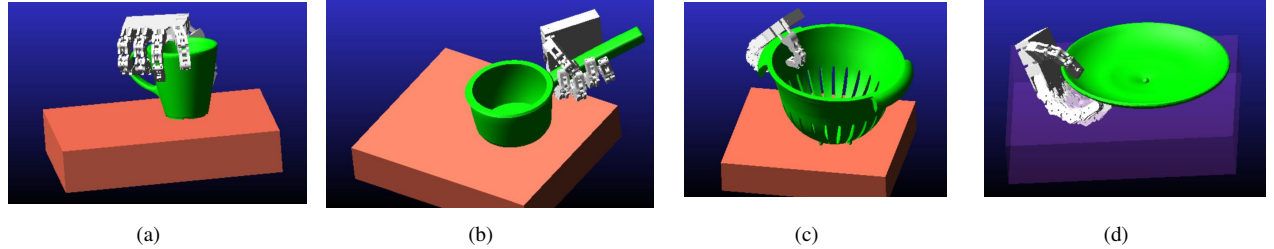


Fig. 8. Examples of stable grasp achieved with the ADAMS simulations. Using the same control command to close the hand, the final joint configuration is determined by the object shape.

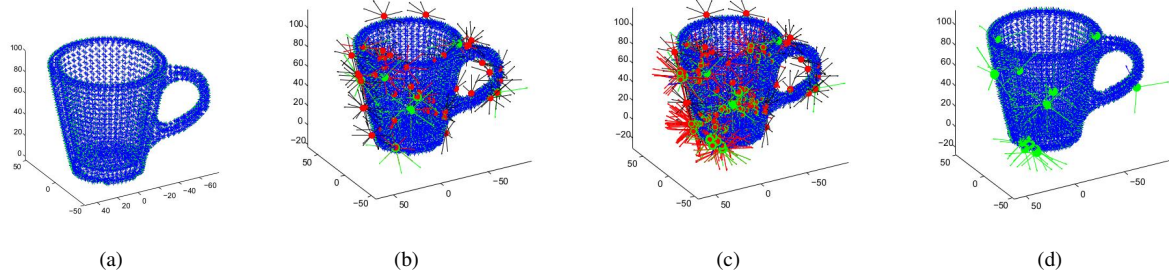


Fig. 9. MATLAB representation of grasping attempt results for the cup. Red points correspond to palm configuration that did not bring to a stable grasp. Green points correspond to successful hand configurations. Fig. (b) shows the results for the first 50 points, Fig. (c) shows the results for all the points tested. Fig. (d) shows only successful configurations.

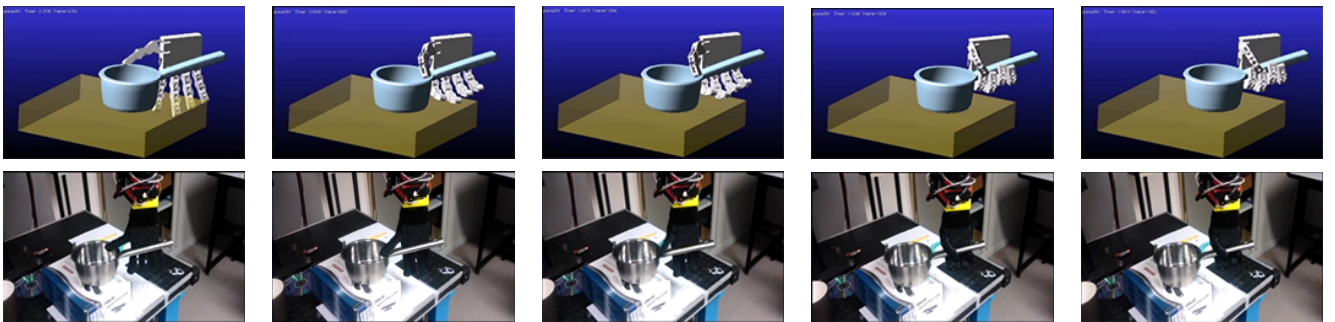


Fig. 10. A snapshot sequence for the pot, comparing the simulation results and the experiment performed with the Pisa/IIT SoftHand prototype.

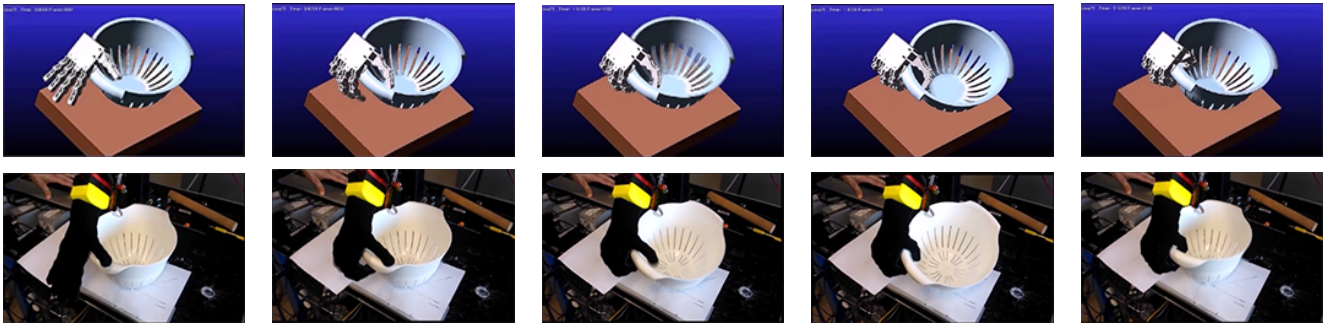


Fig. 11. A snapshot sequence for the colander, comparing the simulation results and the experiment performed with the Pisa/IIT SoftHand prototype.

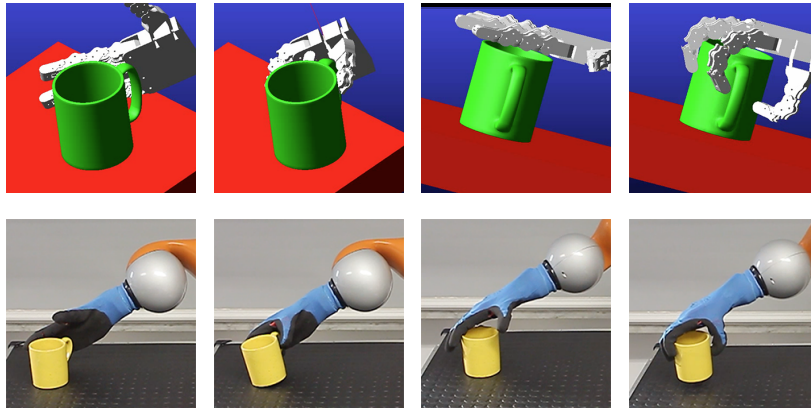


Fig. 12. A possible application of the analysis tool: the top four panels show some grasps that were found in simulation, and the bottom four panels show the same grasps implemented in the SoftHand attached to a KUKA lightweight robot.

- [3] C. Rosales, R. Suarez, M. Gabicci, and A. Bicchi, "On the synthesis of feasible and prehensile robotic grasps," in *Robotics and Automation (ICRA), 2012 IEEE International Conference on*, 2012, pp. 1–7.
- [4] M. Teichmann and B. Mishra, "Reactive algorithms for grasping using a modified parallel jaw gripper," in *Robotics and Automation, 1994. Proceedings., 1994 IEEE International Conference on*, 1994, pp. 1–6.
- [5] R. Platt, A. H. Fagg, R. A. Grupen, W. Bluethmann, R. Ambrose, M. Diftler, E. Huber, A. Fagg, M. Rosenstein, R. Grupen, C. Breazeal, A. Brooks, A. Lockerd, R. A. Peters, O. C. Jenkins, M. Mataric, and M. Bugajska, "Null-Space Grasp Control: Theory and Experiments," *Robotics, IEEE Transactions on*, no. 2, pp. 1–14, 2010.
- [6] D. Wang, B. Watson, and A. Fagg, "A switching control approach to haptic exploration for quality grasps," in *Proceedings of the Workshop on Robot*, Jan. 2007, pp. 1–8.
- [7] Robotiq, "Robotiq adaptive gripper: Specification sheet," Jun. 2014. [Online]. Available: <http://robotiq.com/en/>
- [8] R. Deimel and O. Brock, "A compliant hand based on a novel pneumatic actuator," in *Robotics and Automation (ICRA), 2013 IEEE International Conference on*. IEEE, 2013, pp. 2047–2053.
- [9] ———, "A novel type of compliant, underactuated robotic hand for dexterous grasping," in *Proceedings of Robotics: Science and Systems*, Berkeley, USA, July 2014.
- [10] L. U. Odhner, L. P. Jentoft, M. R. Claffee, N. Corson, Y. Tenzer, R. R. Ma, M. Buehler, R. Kohout, R. D. Howe, and A. M. Dollar, "A compliant, underactuated hand for robust manipulation," *The International Journal of Robotics Research*, vol. 33, no. 5, pp. 736–752, 2014.
- [11] M. G. Catalano, G. Grioli, E. Farnioli, A. Serio, C. Piazza, and A. Bicchi, "Adaptive synergies for the design and control of the pisa/iit softhand," *International Journal of Robotics Research*, vol. 33, p. 768–782, 2014.
- [12] K. Hsiao, S. Chitta, M. Ciocarlie, and E. G. Jones, "Contact-reactive grasping of objects with partial shape information," in *Intelligent Robots and Systems (IROS), 2010 IEEE/RSJ International Conference on*, 2010, pp. 1–8.
- [13] E. Klingbeil, D. Rao, B. Carpenter, V. Ganapathi, A. Y. Ng, and O. Khatib, "Grasping with application to an autonomous checkout robot," *2011 IEEE International Conference on Robotics and Automation*, pp. 2837–2844, May 2011.
- [14] F. T. Pokorny, J. A. Stork, and D. Kragic, "Grasping objects with holes: A topological approach," *Proceedings - IEEE International Conference on Robotics and Automation*, pp. 1100–1107, 2012.
- [15] L. Montesano, M. Lopes, A. Bernardino, J. Santos-Victor, F. S. Melo, and R. Martinez-Cantin, "Learning grasping affordances from local visual descriptors," in *Development and Learning, 2009. ICDL 2009. IEEE 8th International Conference on*, 2009, pp. 1–6.
- [16] R. Detry, E. Bašeski, M. Popović, and Y. Touati, "Learning continuous grasp affordances by sensorimotor exploration," *From motor learning to*, Jan. 2010.
- [17] J. Bohg and D. Kragic, "Learning grasping points with shape context," *Robotics and Autonomous Systems*, vol. 58, no. 4, pp. 362–377, Apr. 2010.
- [18] A. Saxena, J. Driemeyer, and A. Y. Ng, "Robotic Grasping of Novel Objects using Vision," *The International Journal of Robotics Research*, vol. 27, no. 2, pp. 157–173, Feb. 2008.
- [19] A. Bierbaum and M. Rambow, "Grasp affordances from multi-fingered tactile exploration using dynamic potential fields," *Humanoid Robots*, Jan. 2009.
- [20] A. Herzog, P. Pastor, M. Kalakrishnan, L. Righetti, J. Bohg, T. Asfour, and S. Schaal, "Learning of grasp selection based on shape-templates," *Autonomous Robots*, vol. 36, no. 1-2, pp. 51–65, 2013.
- [21] M. ADAMS. (2014, Jan.) Msc software last accessed. [Online]. Available: <http://web.mscsoftware.com/>
- [22] A. T. Miller, S. Knoop, H. I. Christensen, and P. K. Allen, "Automatic grasp planning using shape primitives," *2003 IEEE International Conference on Robotics and Automation (Cat. No.03CH37422)*, pp. 1824–1829, Jan. 2003.
- [23] R. Diankov and J. Kuffner, "Openrave: A planning architecture for autonomous robotics," *Robotics Institute, Pittsburgh, PA, Tech. Rep. CMU-RI-TR-08-34*, pp. 1–18, Jan. 2008.
- [24] B. León, S. Ulbrich, R. Diankov, G. Puche, M. Przybylski, A. Morales, T. Asfour, S. Moisio, J. Bohg, J. Kuffner, and R. Dillmann, *OpenGRASP: A Toolkit for Robot Grasping Simulation*. Springer Berlin Heidelberg, Jan. 2010.